

Hydrofoils: Optimum Lift-Off Speed for Sailboats

Abstract. For a hydrofoil sailboat there is a unique optimum lift-off speed. Before this speed is reached, if there are no parasitic vertical hydrofoil appendages, the submerged or partially submerged hydrofoils increase drag and degrade performance. As soon as this speed is reached and the hydrofoils are fully and promptly deployed, the performance of a hydrofoil-borne craft is significantly improved. At speeds exceeding optimum lift-off speed, partially submerged hydrofoils impair performance if there is no significant effect of loading on the hydrofoil lift-to-drag ratio.

As noted by Chance *et al.* (1), "It seems now that science and sailing sport may go hand in hand to give one of nature's most exhilarating physical experiences an intellectual aspect as well." Application of scientific sailing principles is not, however, new. In 1714, Johann Bernoulli resolved, albeit not rigorously, a dispute between Huygens and Chevalier Renau (Chief Marine Engineer to Louis XIV) on the best sail angle and tack for ships, given the wind velocity relative to the ship's velocity. Unfortunately, few scientific principles have been applied to sailcraft in the last two centuries. Modern-day sailcraft, having radically new designs, now encourage the formulation and application of new scientific principles. An especially interesting aspect of modern-day sailing is the use of hydrofoil suspension (2). In a conventional hydrofoil power boat, lift-off on the foils is achieved by brute-force increase in propulsive thrust; since the boat is ordinarily limited only in the total amount of energy that it can expend, and since its propulsion system can be designed with sufficient thrust to achieve lift-off, impairment of performance before lift-off with the hydrofoils already deployed (submerged) is not especially crucial. In hydrofoil-borne sailcraft, on the other hand, one is ordinarily limited as to thrust (the energy derived from the winds may be variable, but this variability imposes no real long-term limitation). This limitation in thrust is especially severe in light and moderate winds; submergence of the sailcraft's hydrofoils, before lift-off, often creates so much excess hydrodynamic drag that the craft may not even reach a speed sufficient for lift-off on the foils. The question then arises of what optimum speed of hydrofoil submergence yields the lowest drag-

force profile for the craft as a function of its speed.

Figure 1 is a typical plot of craft drag force (f_D) as a function of craft speed (V) for a craft having no parasitic vertical hydrofoil appendages (such as rudders or center boards) and for which no significant variation in hydrofoil lift:drag ratio results from hydrofoil loading. Curve A shows the drag of a buoyant hull alone. Curves B_1 and B_2 show the drag of a buoyant hull having its hydrofoils continuously in the water. There are two branches to curve B: B_1 involves a lift-off speed (\bar{V}_{l_o}) less than the optimum lift-off speed ($\bar{V}_{l_o}^*$) (low-speed lift-off; hydrofoil area therefore larger than optimum), and B_2 involves a lift-off speed greater than the optimum lift-off speed (high-speed lift-off; hydrofoil area therefore smaller than optimum).

Simple numerical calculations show that, even when the hull is partially raised from the water by the hydrofoils, hull drag plus hydrofoil drag are always greater than the drag of the hull alone for $\bar{V}_{l_o} < \bar{V}_{l_o}^*$, and greater than the drag of the hydrofoils alone (hull suspended above the water) for $\bar{V}_{l_o} > \bar{V}_{l_o}^*$. Even if the area of the continuously submerged hydrofoils is designed to achieve lift-off at $\bar{V}_{l_o}^*$, the drag remains always greater for $V < \bar{V}_{l_o}^*$ (premature lift-off), as shown in curve C.

Curve D (Fig. 1) shows the drag of

a buoyant hull of which the hydrofoils are submerged after the optimum lift-off speed (tardy lift-off), and curve E shows the drag of a craft when the hydrofoils are "rapidly" submerged at the optimum lift-off speed. The hydrofoils are assumed to exhibit a lift:drag ratio $[L/D]_h$ that depends on both the fractional load on the hydrofoils, $(V/V_{l_o})^2$, and the craft's speed.

It is clear from Fig. 1 that, if the hydrofoils were designed with an area appropriate to the optimum lift-off speed $\bar{V}_{l_o}^*$, and could be very rapidly submerged at this optimum speed (with the result of negligible decrease in craft speed), the least overall drag would result—that is, the drag profile would follow curve E. One can state that the optimum lift-off speed $\bar{V}_{l_o}^*$ is the speed that minimizes the total power required to accelerate from $V = 0$ to some final craft speed. For simple hydrofoil sailcraft, which exhibit both negligible deceleration and negligible increase in aerodynamic thrust at hydrofoil submergence—that is, at lift-off (or in which these two factors compensate at the lift-off)— $\bar{V}_{l_o}^*$ is the speed at which the hydrofoil-borne operation of the craft requires the same propulsive thrust (or wind) as does its operation when the hydrofoils are not immersed and the craft is borne by a conventional hull (or hulls).

Let us quantitatively define this opti-

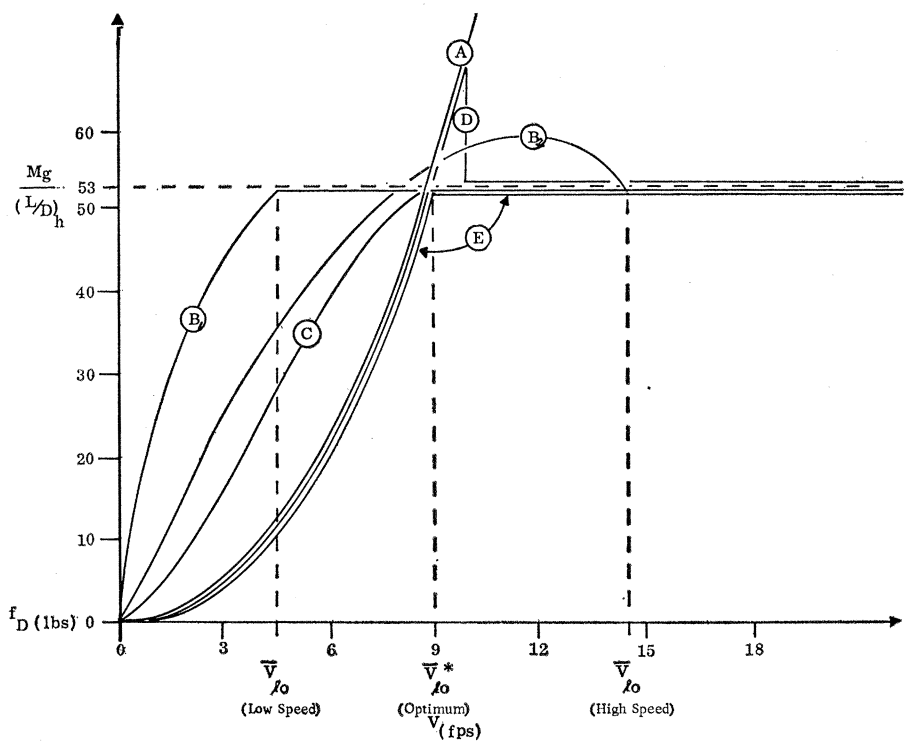


Fig. 1. Plot of typical numerical results for small α and β and for negligible variation of $(L/D)_h$ with V .

mum lift-off speed. The hull drag at optimum lift-off speed (f_{DH}) is (3)

$$f_{DH} = (1/2) \rho_w C_D A_H (V_{l_0}^*)^2 \quad (1)$$

where ρ_w is the density of the water, A_H is the effective area of the hull as measured for computation of the hydrodynamic drag force of the hull, and C_D is the hydrodynamic-drag coefficient of the hull, being taken to be the sum of the frictional-drag coefficient (a function of Reynolds number) and the wave-drag coefficient (a function of Froude number) at the lift-off speed. Let k be the ratio of the effective area of the hull (A_H), as measured for computation of hydrodynamic hull drag, to the two-thirds power of the craft's displacement (Δ); that is, $k = (A_H/\Delta^{2/3})$ as defined at lift-off. By Archimedes principle, $\Delta = M/\rho_w$, where M is the mass of the craft, so that

$$f_{DH} = (1/2) \rho_w k (M/\rho_w)^{2/3} C_D V^2 \quad (2)$$

Let $(L/D)_h$ be the overall lift:drag ratio of the craft, evaluated at lift-off speed $V_{l_0}^*$ when it is hydrofoil-borne (hydrofoils fully loaded). Thus the drag occasioned by the hydrofoils (f_{DF}) is in general

$$f_{DF} = (1/2) \rho_w C_{Dh} A_h V^2 \quad (3a)$$

and when fully hydrofoil-borne it is

$$f_{DF} = Mg/(L/D)_h \quad (3b)$$

where g is the acceleration of gravity, C_{Dh} is the hydrofoil-drag coefficient, and A_h is the submerged area of the hydrofoils. Equating of Eqs. 2 and 3b at $V = V_{l_0}^*$ yields the equation governing the optimum lift-off speed for a simple hydrofoil craft:

$$V_{l_0}^*(V, V_{l_0}) = (2g)^{1/2} (M/\rho_w)^{1/3} / (k C_D (L/D)_h)^{1/2} \quad (4)$$

Since C_D and $(L/D)_h$ are functions of V and V_{l_0} , Eq. 4 implies an evaluation of $V_{l_0}^*(V, V_{l_0})$ at V is equal to $V_{l_0}^*$ in order to yield $\bar{V}_{l_0}^*$. The optimum maximum hydrofoil area ($A_{h \max}$) associated with the optimum speed is given for simple craft by

$$A_{h \max} = 2Mg/\rho_w \bar{C}_{Lh} (\bar{V}_{l_0}^*)^2 \quad (5)$$

where \bar{C}_{Lh} is the overall value for the lift coefficient of the hydrofoils, evaluated at V is equal to $V_{l_0}^*$. [The value of C_{Lh} can be modified by change in the angle of attack of the hydrofoils in order to obtain the largest cavitation-free $(L/D)_h$ as a function of V and loading on the hydrofoils.] As a numerical example, let us consider a typical hydrofoil-borne sailcraft (4) designed by me

in which $M \cong 27$ slugs (875 lb or 32.6 kg), $\rho_w = 2$ slugs per cubic foot or 1025 kg/m³ (salt water), $k = 5.7$, $C_D = 0.02$, $(L/D)_h = 16.5$, so that

$$\begin{aligned} \bar{V}_{l_0}^* &= [(2) (32)]^{1/2} (27/2)^{1/3} / \\ &[(5.7) (0.02) (16.5)]^{1/2} = 9 \text{ ft/sec} \\ &(2.74 \text{ m/sec}) \cong 5 \text{ knots} \end{aligned}$$

Such a low lift-off speed, attainable in a breeze of about 12 knots, would be very difficult to achieve if the hydrofoils were not submerged at the optimum lift-off speed and if their maximum area and lift coefficient were not designed to lift the craft off at optimum lift-off speed.

The area of the hydrofoils, for a lift coefficient of $\bar{C}_{Lh} = 0.95$, is given by

$$A_{h \max} = [(2) (875)/(2) (0.95) (9)^2] = 11.5 \text{ ft}^2 \quad (1.07 \text{ m}^2)$$

Note that the hydrofoil loading at optimum lift-off is relatively small; that is, loading = 875/11.5 = 76 lb/ft² (3.05 kg/m²). Achievement of optimum lift-off speeds exceeding about 15 knots is not very realistic for sailcraft. Solution of Eq. 4 for M , if one assumes a 15-knot limitation in speed, implies that hydrofoil suspension is not practical for sailcraft weighing more than 640,000 lb or 238,000 kg. [Here $C_D (L/D)_h$ is assumed not to change significantly.]

This analysis (5) must be modified if there are parasitic submerged areas A_p , independent of lift-off, that do not vary as $(M/\rho_w)^{2/3} = \Delta^{2/3}$ —such things as rudders and center boards. Analytically, if we define the efficiency of the optimum situation η_1 as the ratio of the drag of hydrofoils plus hull to the drag of the hull alone, it can be shown that for $V \leq V_{l_0} \leq \bar{V}_{l_0}^*$ (curve B_1) and $V \leq V_{l_0}^* \leq V_{l_0}$ (curve B_2) (6)

$$\eta_1(V, V_{l_0}, V_{l_0}^*) = \{[1 - (V/V_{l_0})^2]^{3/2} + [V_{l_0}^*/V_{l_0}]^2\} / (1 + \alpha) \quad (6)$$

where $\alpha = A_p/k(M/\rho_w)^{2/3}$ and

$$V_{l_0}^2 = 2Mg/A_h \rho_w C_{Lh}$$

[$\bar{V}_{l_0} = V_{l_0}$ ($V = V_{l_0}$) that is, evaluated at $V = V_{l_0}$]. The $V_{l_0}^*$ of Eq. 4 and V_{l_0} are considered to be variable as a function of craft speed and the fractional load on the hydrofoils $(V/V_{l_0})^2$. From Fig. 1, $\eta_1 =$ (ordinate of curve B_1, B_2 , or C)/(ordinate of curve E) for $V < \bar{V}_{l_0}^*$. For negligibly small A_p , η_1 always exceeds 1 (7), except when $V = \bar{V}_{l_0}^*$ and there is no value to partial or complete submergence of hydrofoils before the speed $\bar{V}_{l_0}^*$ is reached or for choosing $\bar{V}_{l_0} \neq \bar{V}_{l_0}^*$. The statement is true for either nonoptimum hydrofoil areas such that $\bar{V}_{l_0} \neq V_{l_0}^*$ (curves B)

or optimum hydrofoil areas given by Eq. 5 such that $\bar{V}_{l_0} = \bar{V}_{l_0}^*$ (curve C). On the other hand, if A_p is an appreciable fraction of $k\Delta^{2/3}$, then there could be an advantage to the submergence of hydrofoils prior to the craft reaching the critical lift-off speed $\bar{V}_{l_0}^*$.

The second efficiency ratio of interest is the ratio of the drag force of a craft with a hydrofoil area smaller than that associated with $\bar{V}_{l_0}^*$, that is $\bar{V}_{l_0} > \bar{V}_{l_0}^*$, plus the hull to the drag force of a craft fully elevated on its hydrofoils with an optimum hydrofoil area yielding $\bar{V}_{l_0} = \bar{V}_{l_0}^*$. This efficiency ratio is termed η_2 , and it can be shown that for $V_{l_0}^* \leq V \leq V_{l_0}$ (8)

$$\eta_2(V, V_{l_0}, V_{l_0}^*) = (V/V_{l_0}^*)^2 [1 - (V/V_{l_0})^2]^{2/3} + \{(V/V_{l_0})^2\} \{1 - \beta[1 - (V/V_{l_0})^2]\} \quad (7)$$

where $1 - \beta$ is the ratio of lift:drag of the fully loaded ($V = V_{l_0}$) to completely unloaded ($V/V_{l_0} = 0$) hydrofoil. From Fig. 1, $\eta_2 =$ (ordinate of curve B_2)/(ordinate of curve E) for $V > \bar{V}_{l_0}^*$. If we assume $\beta[1 - (V/V_{l_0})^2] \ll 1$, then for the range $\bar{V}_{l_0}^* \leq V \leq \bar{V}_{l_0}$, $\eta_2 > 1$ except for $V = \bar{V}_{l_0} = \bar{V}_{l_0}^*$ at which point $\eta_2 = 1$. (see curves B, D , and E for $V \geq \bar{V}_{l_0}^*$ in Fig. 1.) Thus, there is no advantage to be gained by operating a craft on hydrofoils having an area different from that which yields $\bar{V}_{l_0}^*$, unless there is a significant difference in hydrofoil lift-to-drag ratio as the loading on the hydrofoil changes.

In the case of the efficiency ratio η_1 , β has no meaning since a partially submerged hydrofoil is always assumed (including the effects of speed and loading); but in the efficiency ratio η_2 , α has no meaning since the parasitic area is always included in the $(L/D)_h$ ratio.

Four basic principles can be defined:

1) There is a unique optimum lift-off speed for any given water conveyance (hydrofoil) craft, which can be approximately computed from Eq. 4, where all the coefficients are evaluated at $V = \bar{V}_{l_0}^*$.

2) It is of no value to employ hydrofoils having a maximum area different from that associated with the optimum lift-off speed as approximately computed from Eq. 5.

3) Before a water-conveyance (hydrofoil) craft reaches the optimum lift-off speed, there is no value to be gained by the use of hydrofoils in combination with a partially elevated craft unless there are appreciable parasitic submerged areas independent of hydrofoil submergence (in fact, the performance of

a craft is ordinarily degraded if hydrofoils of any area are immersed at a craft speed less than the optimum lift-off speed).

4) After a water-conveyance (hydrofoil) craft has reached the optimum lift-off speed, there is no value to be gained by the use of hydrofoils in combination with a partially elevated craft unless there is a significant variation in $(L/D)_h$ due to hydrofoil loading [in fact, the performance of a craft is ordinarily degraded if any portion of the hull(s) is submerged at a craft speed greater than the optimum lift-off speed].

ROBERT M. L. BAKER, JR.
Computer Sciences Corporation and
University of California, Los Angeles

References and Notes

1. B. Chance, Sr., P. DeSaix, H. Herreshoff, J. H. Milgram, *Science* **156**, 412 (1967).
2. H. M. Barkla, *Trans. Roy. Inst. Naval Architects, London* **93**, 247 (1951); K. S. M. Davidson, *Surveys in Mechanics* (Cambridge Univ. Press, London, 1956), p. 473; B. Smith, *The 40-Knot Sailboat* (Grosset and Dunlap, New York, 1963), pp. 1-134; C. A. Marchaj, *Sailing Theory and Practice* (Dodd, Mead, New York, 1964), pp. 305-310; C. Miller, *Rudder* (July 1965), pp. 20-26.
3. Equation 1 is a modification of equation 53, p. 176, of L. Prandtl, *Essentials of Fluid Dynamics* (Haftner, New York, 1952).
4. A conservative and easily achievable $(L/D)_h$ was chosen from data given in R. Altmann, *High-Speed Towed Hydrofoil Sled, Amer. Inst. Aero. Astronaut. and Soc. Nav. Architects and Mar. Engr., Advanced Marine Vehicles Meeting*, May 1967, p. 3 and Fig. 1.
5. W. S. Bradfield, private communication, 5 May 1968.
6. The algebra that results in Eq. 6 is based upon an addition of Eqs. 2 and 3a [where $M/\rho w$ is replaced here by $[Mg - f_{DF} (L/D)_h]/\rho w g$ and $(L/D)_h$ is assumed to include A_p and be a function of craft speed and hydrofoil loading] and a division of this sum by Eq. 2 plus $(1/2) \rho w A_p C_D V^2$. For certain hull forms, k and C_D vary with Δ , and this effect can be included by multiplying the term $[1 - (V/V_{i_0})^2]^{2/3}$ in Eq. 6 by the linearized $[1 - \alpha_1 (V/V_{i_0})^2]$ where α_1 is the fractional increase or decrease (if negative) in kC_D between $\Delta \rightarrow 0$ and $\Delta = M/\rho w$.
7. If $(L/D)_h$ and C_D vary significantly with V , for example, according to the linearized approximation

$$C_D(V) \cong C_D(V = \bar{V}_{i_0}^*) [1 + \delta (V - \bar{V}_{i_0}^*)]$$
and

$$(L/D)_h(V) \cong (L/D)_h(V = \bar{V}_{i_0}^*) [1 - \beta_1 (V - \bar{V}_{i_0}^*)]$$
then

$$(V_{i_0}^*)^2 \cong (\bar{V}_{i_0}^*)^2 [1 - (\delta - \beta_1) (V - \bar{V}_{i_0}^*)]$$
where, ordinarily, $\delta > \beta_1$. Where η_1 applies ($V \leq \bar{V}_{i_0}^*$), $V_{i_0}^* > \bar{V}_{i_0}^*$ and where η_2 applies ($\bar{V}_{i_0}^* < V$), $V_{i_0}^* < \bar{V}_{i_0}^*$. In either case the appropriate η exhibits a larger value than it would have without the δ and β_1 effect. Since $\delta - \beta_1$ is small, $V_{i_0}^* \cong \bar{V}_{i_0}^*$ in any event.
8. The algebra that results in Eq. 7 is based on an addition of Eqs. 2 and 3a (where, again, $M/\rho w$ is replaced by $[Mg - f_{DF} (L/D)_h]/\rho w g$ and A_p is accounted for in $(L/D)_h$) and a division of this sum by Eq. 3b with $(L/D)_h$ taken to be the fully loaded hydrofoil value and related to an arbitrarily loaded hydrofoil by the linearized (approximate) relationship $(L/D)_h$ (fully loaded) = $(L/D)_h \{1 - \beta [1 - (V/V_{i_0})^2]\}$.
9. Research supported entirely by Transportation Sciences Corporation, Los Angeles, California.

18 June 1968

13 DECEMBER 1968

Mercury's Rotation Period: Photographic Confirmation

Abstract. *Photographic measures of surface features on Mercury have led to a rotation period of 58.663 ± 0.021 days, which is in good agreement with the 58.646-day period required by a predicted 2:3 resonance between the axial and orbital periods. The incorrect interpretation of earlier visual and photographic observations which supported an 88-day rotation period appears to be partially explained by peculiar characteristics associated with the observability of various hermetic longitudes. The apparent contrast of most of the recorded surface features is marginal for visual observation when viewed through the terrestrial daytime sky. The intrinsic contrast of a relatively conspicuous feature was measured as 0.20, a value lower than that of typical markings observed on the moon and Mars.*

Throughout most of this century we have unhesitatingly accepted 88 days as the axial rotation period of the planet Mercury, or with somewhat less certainty 87.969 days, an interval precisely equal to its period of orbital revolution about the sun. This 88-day rotation period was first announced by Schiaparelli (1) after 8 years of visual observations through his modest telescope. Repeated confirmation was given (1) over the next several decades, but the matter was considered settled when Antoniadi published his support of the 88-day period (2). Still further confirmation was submitted by Dollfus (3) in the form of both visual and photographic evidence obtained at the French high-altitude observatory at Pic-du-Midi. The optical interpretation did not stand alone; theoretical arguments suggested that solar gravitational forces acting on a tidal deformation would lock Mercury's axial and orbital periods into synchronism in a manner similar to that of the moon in its orbit about the earth (2).

In 1965 Pettengill and Dyce announced that their radar observations of Mercury gave evidence for a rotation period of 59 ± 5 days (4). Furthermore Colombo suggested that the rotation period might be equal to exactly $2/3$ of the orbital period, or 58.646 days (5). While improved radar measures continued to converge on the 59-day period, several investigators found theoretical arguments which could account for Mercury's axial rotation being locked

into a 2:3 resonance with its orbital revolution (6).

A closer inspection was made of the earlier visual and photographic records, particularly the observations of Fournier, Antoniadi, Camichel, and Dollfus, which are generally considered to be the most reliable. Cruickshank and Chapman (7) found that certain visibility relations had combined in such a way that the historical records could support either the 88- or 59-day periods, although they assigned greater probability to the latter. Dollfus and Camichel (7) have reported recent visual observations which they contend are consistent only with a rotation period of 58.67 ± 0.03 days. Within the probable error, this period is in complete agreement with the 2:3 resonance condition. We would emphasize that to date all evaluations of the rotation period of Mercury have made use of recurrent appearances of recognizable features on the planet's surface; there are no references to direct quantitative observations of rotational motion.

We initiated our program of photography of Mercury in late 1965. As an object for telescopic photography, Mercury is among the most difficult in the solar system. Never appearing more than 27° (elongation angle) from the sun, its minute disk must usually be photographed in full daylight. Optimum observing geometry requires a compromise between phase and apparent size, and this occurs when the phase angle is approximately 70° . At this phase the elongation angle has an average value of 20° , and the disk is a mere 6 seconds of arc in diameter. The observational difficulty can best be expressed by the limit of our success over the past $2\frac{1}{2}$ years—a total of only 96 useful photographic plates on 64 different dates.

Until March of this year, the results of our photographic program were generally inconclusive, although a pair of plates taken on 6-8 May 1966 strongly suggested the 59-day rotation period. During March and April, however, we obtained several more plate sequences in which the daily rotational motion of several surface features across the disk of Mercury could be detected and measured. Rotation periods for four of these discrete surface features (tentatively labeled A, B, C, and D) are given in Table 1.

The observations summarized in Table 1 support the 59-day rotation period. Making use of the directly derived photographic rotation period,